Inorganic Chemistry

Article

pubs.acs.org/IC

New Ruthenium Nitrosyl Pincer Complexes Bearing an O_2 Ligand. Mono-Oxygen Transfer

Eran Fogler,[‡] Irena Efremenko,[#] Moti Gargir,[‡] Gregory Leitus,[#] Yael Diskin-Posner,[#] Yehoshoa Ben-David,[‡] Jan M. L. Martin,*[,‡] and David Milstein*[,‡]

[‡]Department of Organic Chemistry and [#]Department of Chemical Research Support, Weizmann Institute of Science, Rehovot 76100, Israel

Supporting Information

ABSTRACT: We report on $Ru^{(II)}(\mu^2\text{-}O_2)$ nitrosyl pincer complexes that can return to their original Ru(0) state by reaction with mono-oxygen scavengers. Potential intermediates were calculated by density functional theory (DFT) and a mechanism is proposed, revealing a new type of metal−ligand cooperation consisting of activation of the O_2 moiety by both the metal center and the NO ligand. Reaction of the Ru(0) nitrosyl complex **1** with O_2 quantitatively yielded the crystallographically characterized $Ru^{(II)}$ $(\mu^2\text{-}O_2)$ nitrosyl complex **2**. Reaction of **2** with the mono-oxygen scavengers phosphines or CO gave the Ru(0) complex **1** and phosphine oxides, or the carbonyl complex **3** (**1** trapped by CO) and CO_2, respectively. Reaction of **2** with 1 equiv of phosphine at room temperature or −40 °C resulted in immediate formation of half an equivalent of **1** and 1 equiv of phosphine oxide, while half an equivalent of **2** remained unchanged. Overnight reaction at room temperature of **2** with excess CO (≥3 equiv) resulted in **3** and CO_2 gas as the only products. Reaction of **1** with 1 equiv of mono-oxygen source (dioxirane) at −78 °C yielded the $Ru^{(II)}(\mu^2\text{-}O_2)$ complex **2**. Similarly, reaction of the Ru(0) dearomatized complex **4** with O_2 led to the crystallographicaly characterized $Ru^{(II)}(\mu^2\text{-}O_2)$ complex **5**. Further reaction of **5** with mono-oxygen scavengers (phosphines or CO) led to the Ru(0) complex **4** and phosphine oxides or complex **6** (**4** trapped by CO) and CO_2. When instead only 1 equiv of **5** was reacted with 1 equiv of phosphine at room temperature, immediate formation of half an equivalent of **4** and 1 equiv of phosphine oxide took place, while half an equivalent of **5** remained unchanged. When **5** reacted with an excess of CO (≥3 equiv), complex **6** and CO_2 gas were the only products obtained. DFT studies indicate a new mode of metal−ligand cooperation involving the nitrosyl ligand in the oxygen transfer process.

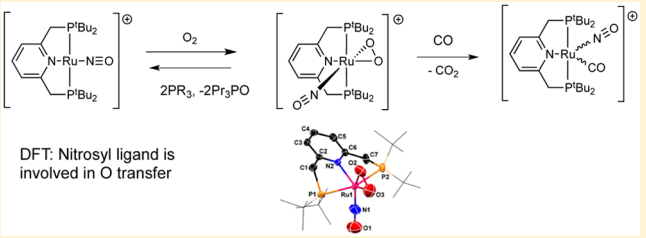

INTRODUCTION

Molecular oxygen can interact with low-valent, electron-rich metal complexes ($[M^n]$) to give the corresponding peroxo complexes and effectively oxidize the metal center by two electrons, yielding $[M^{n+2}](\mu^2\text{-}O_2)$, such as in the reactions of molecular oxygen with $M^{(0)}((PPh)_3)_4$ (M = Ni, Pd, Pt) to give the corresponding $M^{(II)}(\mu^2\text{-}O_2)((PPh)_3)_2$.[1]

Several ruthenium complexes of this type were synthesized, such as $Ru(O_2)(NCS)(NO)(PPh_3)_2$, $RuCl(NO)(\mu^2\text{-}O_2)(PPh_3)_2$, $Ru(\mu^2\text{-}O_2)(CO)_2(PtBu_2Me)_2$, and $Ru(Ph_2PNMeNMePPh_2)_2(\mu^2\text{-}O_2)$.[2−5] Recently even $Ru^{(IV)}(\mu^2\text{-}O_2)$ pincer complexes bearing the dioxygen moiety have been reported.[6]

We have previously reported rhodium *pincer* complexes bearing a dioxygen moiety: $(Me_2C_6H(CH_2P^tBu_2)_2)Rh(O_2)$,[7] and the unusual hydrido-alkene-O_2 complex $RhH(O_2)(CH_2{=}C(CH_2CH_2P^tBu_2)_2)$ formed[8] when a very dilute mixture of O_2 (2 ppm) in argon was bubbled through a solution of $RhH(CH_2{=}C(CH_2CH_2P^tBu_2)_2)$. Pincer ligands can stabilize normally unstable complexes such as the d^6 (PCN)Pt=O complex that was reported by our group.[9] Such oxygen species are potential intermediates in catalytic reactions.

Because of the importance of oxidation reactions with molecular oxygen, several mechanistic studies were performed concerning biological systems[10−12] and homogeneous catalysis.[12−15] Potential catalytic reactions based on these complexes such as[16] formation H_2O_2 from O_2 may replace in the future industrial processes such as the anthraquinone process.[17] This type of oxidation reactions may proceed via terminal oxo intermediates.

Terminal oxo complexes of transition metals are thought to play major roles in various processes, such as catalytic oxidation of organic compounds in chemical and enzymatic processes.[18−25] Since the terminal oxo ligand is a strong p electron donor via the lone electron pairs, it binds most strongly to high-valent early transition metals, such as $Ti^{(IV)}$ and $V^{(V)}$. In these complexes, electrons can delocalize from oxygen into the vacant d orbitals of the metal, and therefore, d^0 to d^2 oxo compounds are common, and the oxo ligand can be ancillary to reactions in the coordination sphere of the metal. Moving from left to right across the Periodic Table, the d orbitals fill up with valence

Received: November 30, 2014
Published: February 19, 2015

DOI: 10.1021/ic502832j
Inorg. Chem. 2015, 54, 2253−2263

electrons, and the oxo ligand becomes destabilized by repulsion.[24,26−29] There are very few terminal oxo complexes with five or more valence d electrons[9,30] (in the past there were several reports on such complexes; however they were retracted[31]). A rare pincer-type, PCN d^6, Pt=O complex was reported by our group.[9]

Several ruthenium pincer-type complexes developed in our laboratory show substantial catalytic activity in various reactions.[32−52] These catalytic reactions may proceed via a new mode of bond activation by metal−ligand cooperation, based on aromatization−dearomatization[53,54] of pyridine- (and acridine)-based pincer complexes that facilitates the activation of chemical bonds.[32−42,45−52,55−61] In the present work, we report O_2 activation by ruthenium nitrosyl pincer complexes that may involve Ru oxo intermediates, including a new type of metal−ligand cooperation involving O_2 activation in which the NO ligand is involved, as supported by density functional theory (DFT) calculations.

RESULTS AND DISCUSSION

We have previously described the synthesis of the Ru(0) complex **1**.[51] This complex reacts immediately with 1 equiv of O_2 or by simple exposure to air to yield complex **2**. In the solid state **2** was stable overnight under a high vacuum, indicating that the O_2 ligand is strongly bound.

Scheme 1. Formation of 2 by Reaction of 1 with O_2

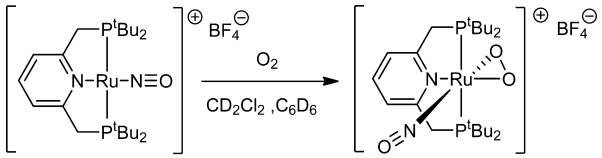

1 **2**

The fully characterized complex **2** gives rise to a singlet at 67.21 ppm in the $^{31}P\{^1H\}$NMR spectrum, and the phosphorus methylene groups of the ligand appear as two multiplets (due to the C_s symmetry of **2**) at 3.74 and 3.44 ppm in the ^1H NMR spectrum. The NO stretch in the IR spectrum appears at 1646.3 cm^{-1} and the O−O stretch appears at 796.4 cm^{-1}. When **2** is prepared with $^{18}O_2$, the $^{18}O-^{18}O$ stretch is shifted to 760 cm^{-1} corresponding to reported values for ruthenium dioxygen compounds.[2,5,62] Complex **2** is unstable toward light and decomposed under Raman measurements.

Crystals suitable for X-ray analysis (containing the BAr^F anion) were obtained by relatively fast (3−4 min, due to the instability of **2** in solution) partial evaporation of an ether solution of **2**. The X-ray structure of **2** reveals a linear NO ligand Ru−N−O angle of 162.8(7)° located trans to the oxygen atom. The Ru−NO bond distance of 1.776(4) Å is almost identical to the reported Ru(II)−NO bond length of 1.775 Å for an analogous pincer complex[51] Ru(PNP)(Cl)$_2$(NO) that was previously reported by us having two chloride atoms cis to each other instead of the two oxygen atoms in **2**. The N−O bond length in **2** (1.201(6) Å) is longer in comparison to Ru(PNP)(Cl)$_2$(NO) (1.123 Å), indicating more back-donation to the NO ligand of **2**. The O−O bond length in the complex (1.395(6) Å) suggests a bond order close to 1, as compared to calculated values at the same level of theory for the O−O bond in H_2O_2 (1.458 Å) and for the O=O bond in O_2 (1.21 Å). Previously reported O−O bond lengths in Ru complexes range between 1.33(2) and 1.47(1) Å.[38−41] The aromatic (rather than dearomatized) structure of **2** is clearly evident in its crystal structure, in which the two hydrogen atoms connected to C1 and C7 were located. In addition, the pairs of bonds C1−C2/C6−C7, C2−C3/C5−C6, C3−C4/C4−C5, and C3−C4/C4−C5 are (within experimental error) of the same length, unlike the expected alternating bond lengths in the putative dearomatized complex.

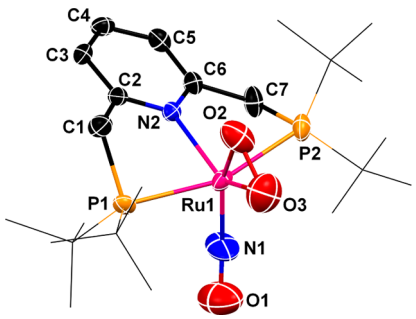

Figure 1. X-ray structure of **2** (ellipsoids shown at 50% probability level). Hydrogen atoms are omitted for clarity. ^{t}Bu groups are presented as wireframe for clarity.

Table 1. Selected Bond Lengths (Å) and Bond Angles (Degree) of Complex 2

O2−O3	1.396(6)	C1−C2	1.494(6)
Ru1−O3	2.012(4)	C6−C7	1.496(6)
Ru1−O2	1.935(4)	C2−C3	1.383(5)
Ru1−N2	2.124(3)	C3−C4	1.372(6)
Ru1−N1	1.776(4)	C4−C5	1.386(6)
N1−O1	1.201(6)	C5−C6	1.385(6)
Ru1−P1	2.404(1)	Ru1−N1−O1	162.8(7)
Ru1−P2	2.433(1)		

The reactivity of **2** toward oxygen scavengers was investigated next. Reacting 2 equiv of **2** with 2 equiv of triethylphosphine at room temperature resulted in immediate formation of 1 equiv of **1** and 2 equiv of triethylphosphine oxide, while 1 equiv **2** remained unreacted. The two oxygen atoms of **2** fully reacted. In order to make sure that this result is not simply due to triethylphosphine dissociation and reaction with free O_2, complex **2** was reacted with 2 equiv of PPh_3, which normally does not react rapidly with free O_2. The result was basically identical, i.e., immediate formation of 1 equiv of **1** and 2 equiv of triphenylphosphine oxide. This result shows that full consumption of the two oxygen atoms on one complex molecule occurred prior to reaction with the O_2 ligand of a second molecule of **2**. We then attempted to monitor this reaction at −40 °C by UV/vis. Surprisingly the reaction reached completion in less than 0.5 s (the minimal time between scans) at −40 °C. This suggests that an intermediate formed on the way from **2** to **1** is more reactive than **2** itself and therefore not observable.

Reaction of **2** at room temperature with 1 equiv of CO resulted in **3** (in an average yield of 36% (out of three experiments, two yielding 30−32% and one 45%, due to the instability of **2**) and a large amount of decomposition products. When **2** was reacted with an excess of CO (≥3 equiv), an unseparable mixture of products forms that converge to give **3** as the only product after being left overnight at room

DOI: 10.1021/ic502832j
Inorg. Chem. 2015, 54, 2253−2263

Scheme 2. Reaction of 2 with Phosphines

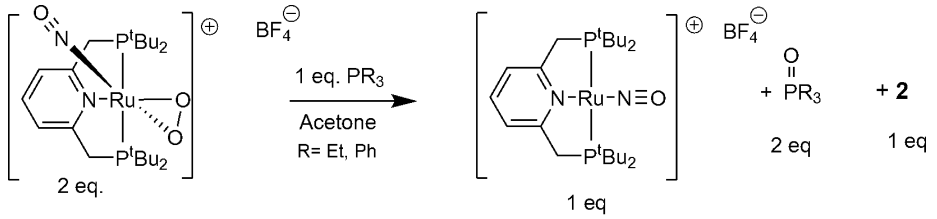

2 1

temperature. IR analysis of the gas phase above the reaction revealed the presence of CO_2 gas.

Scheme 3. Reaction of 2 with CO

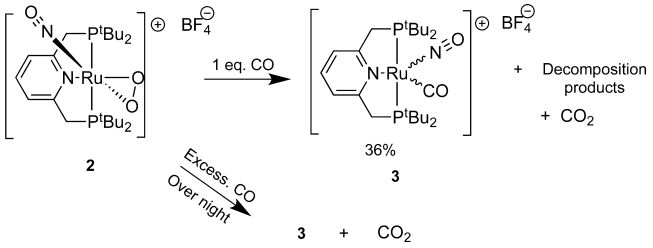

2 3

In order to verify the structure of **3**, it was prepared independently by reaction of **1** with CO and was fully characterized (Scheme 4). Complex **3** gives rise to a singlet at

Scheme 4. Synthesis of 3

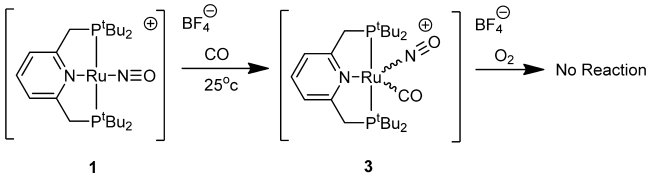

1 3

82.00 ppm in the $^{31}P\{^1H\}$NMR spectrum, and the (Ar)−CH_2−(P) methylene groups of the ligand appear as two multiplets (due to the C_s symmetry of **3**) at 4.44 and 4.28 ppm in the ^1H NMR spectrum. The NO stretch in the IR spectrum appears at 1572 cm^{-1}, while the CO stretch appears at 1940 cm^{-1}.

We surmise that the reaction of **2** with an excess of CO (or with a phosphine) proceeds as follows: upon the addition of CO to a solution of **2**, it reacts with the first two equivalents of CO to give **1** and CO_2. Complex **1** is immediately trapped by CO to give **3**. We believe that the intermediate formed after reaction of **2** with 1 equiv of CO is highly reactive, leading to mainly decomposition products in the absence of a second equivalent of CO.

Next we reacted **1** with mono-oxygen sources. Reaction of **1** with 1 equiv of dioxirane at room temperature led to a complicated mixture of products including **2**. A similar reaction at −34 °C gave a mixture of products including **2** and **1**. Finally this reaction at −78 °C yielded 33−45% of **2** as the only identified product (Scheme 5).

We believe that after transferring one oxygen atom from dioxirane to **1** the intermediate formed is the same as the one formed upon oxygen atom removal from **2** with a phosphine or CO. This intermediate is more activated toward the mono-oxygen source (dioxirane) than **1**, and hence transfer of the second oxygen atom is faster and thermodynamically more favorable with the less stable species (the intermediate) than with the original complex.

Interestingly, the reactivity of **4**[51] is similar to that of **1**. There is no observable interaction or influence of the dearomatized moiety. Upon reaction of **4** with 1 equiv of O_2 or simply by exposure to ambient air complex **5** was immediately formed (Scheme 6). **5** is stable under high vacuum overnight, indicating that the O_2 ligand is strongly bound.

Scheme 6. Synthesis of 5

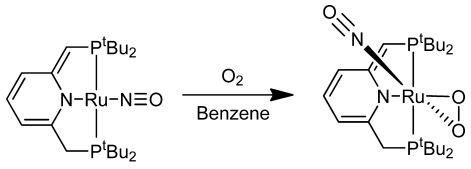

4 5

The fully characterized complex **5** gives rise to two doublets in the $^{31}P\{^1H\}$NMR spectrum at 86.83 and 45.21 ppm (J_{PP} = 344 Hz). In the ^1H NMR spectrum the methylene groups of the ligand appear as a doublet of doublets at 2.85 ppm (J_{HH} = 15.3 Hz, J_{HP} =10.5 Hz) and 2.49 (J_{HH} = 13.5 Hz, J_{HP} =10.5 Hz), and the "arm" vinylic proton appears as a doublet at 3.54 ppm (J_{PH} = 6.3 Hz). The corresponding carbon exhibits a doublet at 68.1 ppm (J_{CP} = 52.3) in the $^{13}C\{^1H\}$ NMR spectrum. The NO stretch in the IR spectrum appears at 1733 cm^{-1}, and the O−O stretch appears at 1021 cm^{-1}. **5** was unstable toward light and decomposed when subjected to Raman measurements.

Single crystals of **5** suitable for X-ray diffraction were obtained by slow evaporation of an ethereal solution of **5**. The

Scheme 5. Reaction of 1 with Dioxirane

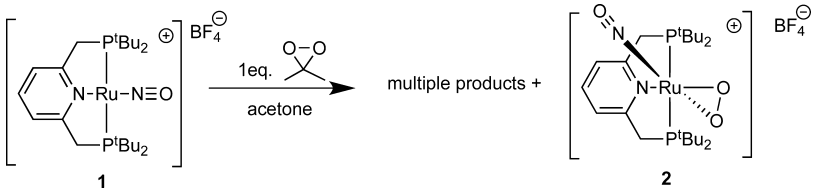

1 2

DOI: 10.1021/ic502832j
Inorg. Chem. 2015, 54, 2253−2263

X-ray structure of **5** reveals a linear NO ligand (Ru−N−O angle of 168.7(2)°) located trans to an oxygen atom. The Ru−NO bond distance (1.752(2) Å) is slightly shorter than the Ru(II)−NO bond (1.777(4) Å) of complex **2**. The N−O bond length in **5** (1.169(2) Å) is slightly shorter than in **2** (1.201(6) Å). This indicates more back-donation to the NO ligand of **2** compared to **5**. The dearomatized structure of **5** is clearly evident in its crystal structure, in which the hydrogen atom connected to C1 was located. In addition, as in the case of **4**, the pairs of bonds C1−C2/C6−C7, C2−C3/C5−C6, C3−C4/C4−C5, and C3−C4/C4−C5 show alternating bond lengths in line with a dearomatized complex.[51] The O−O bond length in **5** of 1.440(2) Å indicates a single bond. It is longer than the O−O bond of 1.396(6) Å of the cationic complex **2**, indicating higher backbonding to O_2 in the case of the neutral complex **5**.

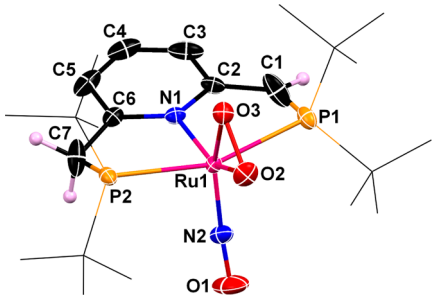

Figure 2. X-ray structure of **5** (ellipsoids shown at 50% probability level). Hydrogen atoms (except for the methylene and vinylic protons) are omitted for clarity. ^{t}Bu groups are presented as a wireframe for clarity.

Table 2. Selected Bond Lengths (Å) and Bond Angles (deg) of 5

Ru1−O2	2.012(1)	C1−C2	1.408(3)
Ru1−O3	1.970(1)	C6−C7	1.454(3)
O2−O3	1.440(2)	C2−C3	1.420(3)
Ru1−P1	2.4163(5)	C5−C6	1.394(3)
Ru1−P2	2.4263(5)	C3−C4	1.364(4)
Ru1−N1	2.095(2)	C4−C5	1.386(4)
Ru1−N2	1.752(2)	Ru1−N2−O1	168.7(2)
N2−O1	1.169(2)		

The relatively long O−O bond in **5** suggested that it might react with electrophiles. However, no reaction was observed with methyl iodide at rt, and when the mixture was heated to 60 °C for 1.5 h the only product was the oxidized ligand. Complex **5** was also inert to hexamethyldisilane at rt, and upon heating to 60 °C a small amount of **5** decomposed to give the oxidized ligand.

Next, we checked the reactivity of **5** with a phosphine as an oxygen scavenger. As observed with complex **2**, reaction of **5** with 1 equiv of PPh_3 resulted in immediate formation of half an equivalent of **4**, half an equivalent of unreacted **5**, and 1 equiv of $OPPh_3$ (Scheme 7). This result indicates full consumption of both oxygen atoms of one molecule of **5** prior to reaction with the dioxygen ligand of a second complex molecule. It also suggests that an intermediate (probably mono-oxo) is formed, which is more reactive than **5** and therefore cannot be detected. Hoping to be able to detect it, by sterically hindering its further oxygen transfer reactivity, we chose to react it with the bulky tri-*tert*-butylphosphine.

Reaction of 2 equiv of **5** with 2 equiv of ^{t}Bu$_3$P at room temperature was very slow (in contrast to the immediate reaction of PPh_3), and after 3 days 1 equiv of **4** and 1 equiv of unreacted **5** were obtained; in addition two singlet peaks in the observed ^{31}P[^{1}H] NMR spectrum indicate formation of unidentified compounds. Thus, ^{t}Bu$_3$P reacted fully with both the oxygen atoms of **5**; additionally, ^{t}Bu$_3$P is more reactive toward free oxygen then PPh_3, and the faster reaction of the latter (immediate vs 3 days) supports the notion that the O_2 ligand is activated by the metal center. Unfortunately, the mono-oxo intermediate was not observed.

Next, the reactivity of **5** toward CO was examined, leading to similar results as in the case of **2**. Reaction of **5** with 1 equiv of CO resulted in unidentified decomposition products, whereas the same reaction using excess (3 equiv) of CO led to an inseparable mixture of products, which when left overnight at room temperature interconverts to yield **6** as the only product, as shown by ^{31}P NMR and ^{13}C NMR. CO_2 gas was detected by IR analysis of the gas phase.

Scheme 8. Reaction of 5 with CO

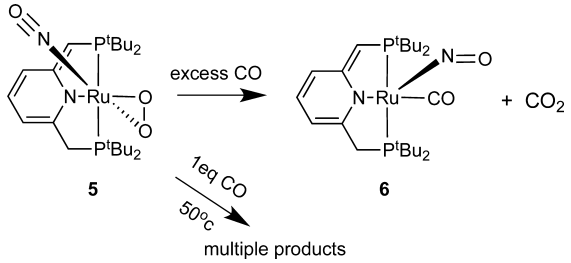

Complex **6** was also prepared independently by the reaction of **4** with CO (Scheme 9) and was fully characterized, including by X-ray diffraction (Figure 3). Pure **6** is not reactive toward O_2.

Scheme 9. Independent Synthesis of 6

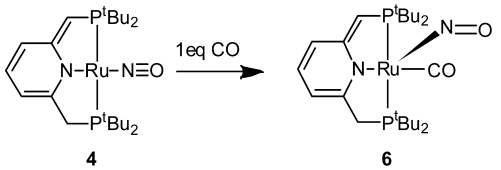

Scheme 7. Reaction of 5 with PPh_3

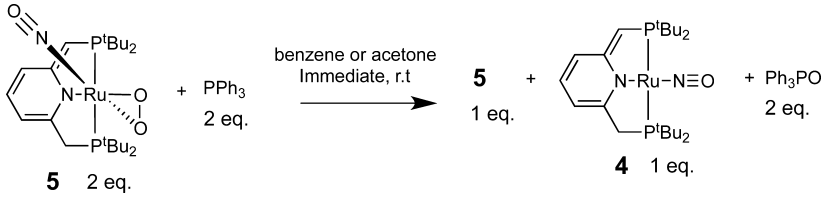

DOI: 10.1021/ic502832j
Inorg. Chem. 2015, 54, 2253−2263

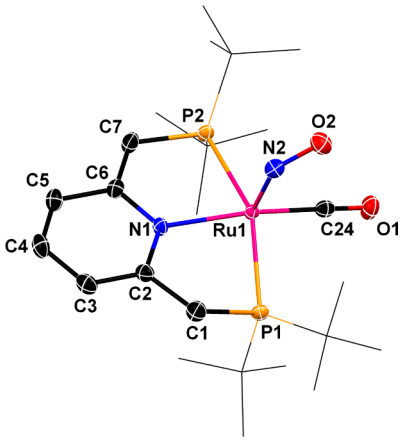

Figure 3. X-ray structure of **6** (ellipsoids shown at 50% probability level). Hydrogen atoms are omitted for clarity. ^{t}Bu groups are presented as a wireframe for clarity.

The fully characterized complex **6**-^{13}CO gives rise to two doublets of doublets in the ^{31}P{^{1}H}NMR spectrum at 82.68 and 81.18 ppm (J_{PP} = 154.0 Hz, J_{PC} = 12.0 Hz). In the ^{1}H NMR spectrum of **6**-^{13}CO the methylene groups of the ligand appear as a doublet of doublets at 2.99 ppm (J_{HH} = 16.4 Hz, J_{HP} = 6.0 Hz), and the "arm" vinylic proton appears as a doublet at 3.61 ppm. (J_{HP} = 3.0 Hz). The corresponding carbon exhibits a doublet of doublets at 62.4 ppm (J_{CP} = 46.6 Hz, J_{CC} = 6.5 Hz), and the CO gives rise to broad singlet at 208.5 ppm in the ^{13}C{^{1}H} NMR spectrum of **6**-^{13}CO. The NO stretch in the IR spectrum appears at 1558 cm^{-1}, and the C−O stretch appears at 1941 cm^{-1}, similar to the N−O stretch of 1570 cm^{-1} and the C−O stretch of 1914 cm^{-1} for the analogous square pyramidal[63] Ru(FBF$_3$)(CO)(bent-NO)(P^{t}Bu$_2$Me)$_2$.

Single crystals of **6** suitable for X-ray diffraction were obtained by cooling a toluene solution of **6** to −70 °C for a few hours. The X-ray structure of **6** reveals a square pyramidal structure with a bent NO ligand, (Ru1−N2−O2 angle 131.1(2)°) located in the apical position, similar to the angle of 135.6° in the analogous square pyramidal Ru(FBF$_3$)(CO)(bent-NO)(P^{t}Bu$_2$Me)$_2$.[63] The Ru−NO bond length of 1.858 (2) Å is slightly longer as compared with the Ru−NO bond length of 1.839 Å in Ru(FBF$_3$)(CO)(bent-NO)(P^{t}Bu$_2$Me)$_2$. The N−O bond length of **6** (1.202(3) Å) is slightly longer as compared with that of Ru(FBF$_3$)(CO)(bent-NO)(P^{t}Bu$_2$Me)$_2$)[63] (1.190 Å). This indicates less back-donation to the NO ligand of **6**. The CO ligand is located trans to the pyridine nitrogen with the Ru−CO bond length of 1.848(2) Å, longer than the corresponding bond ((1.802 Å) of Ru(FBF$_3$)(CO)(bent-NO)(P^{t}Bu$_2$Me)$_2$.[63] The dearomatized structure of **6** is clearly evident in its crystal structure, in which the hydrogen atom connected to C1 was located. In addition, similar to **4** and **5**, the pairs of bonds C1−C2/C6−C7, C2−C3/C5−C6, C3−C4/C4−C5, and C3−C4/C4−C5 exhibit alternating bond lengths.[51]

We believe that the reaction of **5** with excess of CO proceeds as follows: **5** reacts first with 2 equiv of CO to give **4** (and CO_2), which is immediately trapped by CO to give **6**.

COMPUTATIONAL RESULTS

In order to better understand the experimental results, we analyzed the electronic structure of complex **2** and its reactivity toward CO using accurate quantum chemical calculations. The

Table 3. Selected Bond Lengths (Å) and Bond Angles (deg) of 6

Ru1−P2	2.3822(6)	C6−C7	1.386(3)
Ru1−P1	2.3742(6)	C2−C3	1.367(3)
Ru1−N1	2.143(2)	C5−C6	1.436(3)
Ru1−C24	1.848(2)	C3−C4	1.411(4)
Ru1−N2	1.858(2)	C4−C5	1.352(4)
N2−O2	1.202(3)	Ru1−N2−O2	131.1(2)
C1−C2	1.512(3)	Ru1−C24−O1	177.4(2)

virtually square planar structure of **1**, with the NO ligand trans to the aromatic ring, favors its strong π acceptor character. QTAIM analysis shows that the Ru−N bond is a double bond with a delocalization index DI_{Ru-N} = 1.64, while the total charge on the NO ligand of −0.38. Initial weak end-on interaction of incoming O_2 molecule with Ru reduces the symmetry of O_2 π orbitals and favors its "transformation" to the singlet state.[64] It also causes bending of the complex and corresponding stabilization of the d_{z^2} orbital and destabilization of the Ru d_{yz} orbital, such that for ∠N2−Ru−N1 smaller than 120°[65] this orbital becomes the HOMO (Scheme 11). Electron transfer from this MO to the empty π^* orbital of O_2 results in the formation of the closed-shell Ru$^{(II)}$(μ^2-O_2) complex.

Formation of **2** (Scheme 10) is accompanied by a room temperature energy gain of 15.9 kcal/mol in dichloromethane

Scheme 10. Qualitative Representation of Orbital Interactions Leading to the Formation of Complex 2

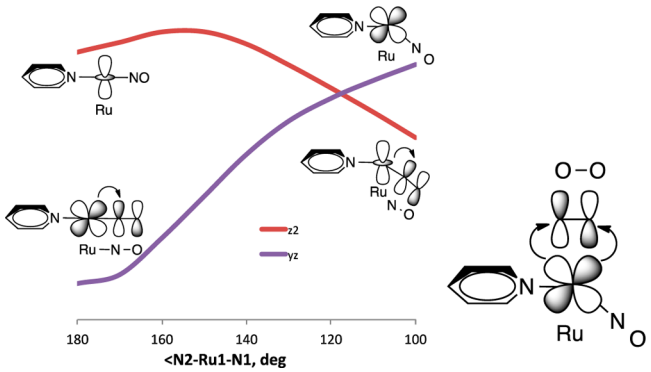

and 16.4 kcal/mol in acetone. The optimized geometry of **2** accords well with the X-ray structure (Table 1S in Supporting Information). Two O atoms in this complex are not equivalent with Ru−O bond lengths of 1.937 and 2.013 Å (Table 1). QTAIM analysis indicates they correspond to a double and a single bond, respectively, with delocalization indices DI_{Ru-O} ("QTAIM bond orders") of 1.78 and 0.73, respectively, while the total negative charge on O_2 ligand of −1.01 (see SI). The triplet state of **2** is 31.1/31.5 kcal/mol higher in energy in dichloromethane/acetone and possesses the Ru$^{\bullet}$-OO^{-} interaction rather that η^2-O_2 bonding.

Inner-sphere O_2 dissociation in **2** has prohibitively high activation barriers in both singlet and triplet states (Figure 4) and leads to O atom transfer to NO (complex **I**). This reaction is slightly exergonic in the triplet state (complex $\mathbf{I}_T$), which again could be better represented as Ru$^{\bullet}$-O^{-} than as an oxo complex. Formation of two oxo ligands was found only on the triplet PES, and it is accompanied by a strong increase in energy (ΔG_{298} = 54.2 kcal/mol). Thus, complex **2** is stabilized

DOI: 10.1021/ic502832j
Inorg. Chem. 2015, 54, 2253−2263

Scheme 11. Two Possible Ways of CO Coordination with 2 and Key Optimized Geometric Parameters of the Complexes

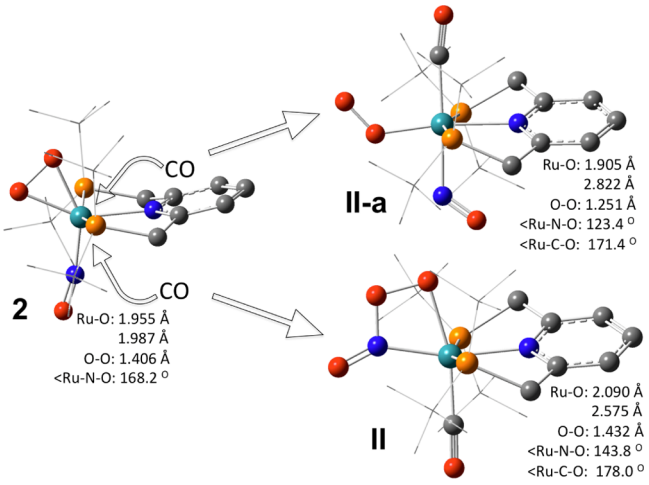

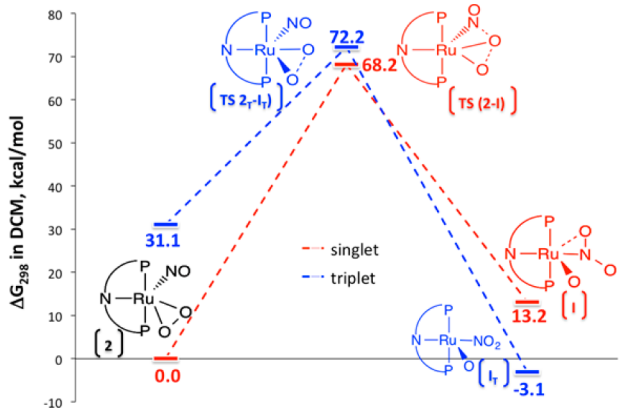

Figure 4. Calculated reaction profiles for O−O bond dissociation in the monocationic complex **2** in singlet and triples states in dichloromethane (DCM).

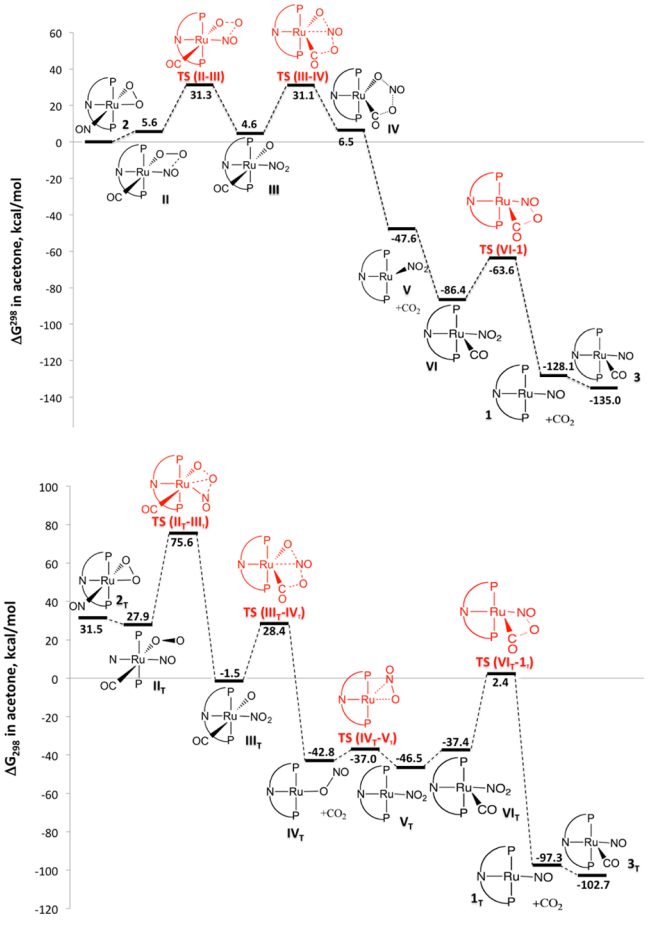

Figure 5. Reaction profiles for CO oxidation by complex **2** in the singlet (top) and triples (bottom) states calculated at the DSD-PBEB95/TZVP(P) level of theory. All the complexes are monocationic; the "+" sign is omitted for clarity.

kinetically, and O−O breaking does not occur in the absence of a reductant.

CO coordination to **2** at the side of O atom is energetically strongly unfavorable (ΔG_{298} = +48.4 kcal/mol) and causes breaking of one of the Ru−O bonds with formation of a Ru−O−O$^{\ominus}$ moiety. In spite of numerous efforts we did not find a transition state for direct coupling between coordinated CO and O ligands. CO coordination at the side of NO leads to NO movement into the plane of the complex accompanied by nonactivated breaking of one Ru−O bond and formation of a new N−O bond (complex **II**). Strong Ru → CO π-backdonation in this complex (Q_{CO} = −0.17 and $DI_{Ru\text{-}CO}$ = 1.37) markedly weakens the Ru−NO bond ($DI_{Ru\text{-}NO}$ decreases from 1.64 in **2** to 0.79 in **II**). Consequently, O−O bond breaking is the first of the rate limiting steps. The lowest energy reaction profile initiated by these entrance-channel reactions on the singlet PES and its close triplet analogue calculated at the DSD-PBEB95-D3BJ/TZVP(P) level of theory are shown in Figure 5. The alternative reaction pathways are shown in the Supporting Information.[66]

The formation of the singlet CO adduct **II** is apparently slightly endergonic. This is almost certainly an artifact of the gas-phase RRHO approximation. In the gas phase, the association is significantly negentropic, but in solution translational and rotational degrees of freedom are significantly restricted by the solvent,[67] and as a result the translational and rotational entropy change of an A + B → AB reaction is significantly reduced. A proposed crude approximation[67] for bimolecular reactions would be to ignore the translational and rotational entropy contributions in solution and only consider the vibrational entropy: This is physically analogous to considering instead $A(solvent)_{nA} + B(solvent)_{nB} + \rightarrow (solvent)_n + A(solvent)_{nAB} + (solvent)_{nAB\text{-}nA\text{-}nB}$. As far as translation and rotation movements are in fact not completely suppressed in solution,[68] this approximation is expected to somewhat underestimate the entropy effect. For the formation of **II** this approximation yields an energy gain of 8.4 kcal/mol. Thus, the activation energies of the subsequent monomolecular reactions should be calculated with respect to **II**. This results in the apparent activation energy for O−O bond dissociation via TS(**II**−**III**) of 25.7 kcal/mol, in good agreement with the experimentally observed reaction rate.

The ability of the stable NO radical to interact with O_2 in its ground triplet state to form a peroxo adduct in the gas phase is well-known and a widely applied industrial process (in HNO_3 production).[69] Similar peroxo moieties were found in transition metal complexes. For instance, the coordinated peroxynitrite Co−O−O−NO moiety was formed as an intermediate in the NO oxidation by the oxy-cobolglobin models of the general formula $(NH_3)Co(Por)(O_2)$ at cryogenic temperatures.[70] The Cu(I)-NO complex was shown to generate a peroxynitrite

DOI: 10.1021/ic502832j
Inorg. Chem. 2015, 54, 2253−2263

(O=NOO$^-$)−Cu(II) species when exposed to oxygen.[71] The oxidation of a nitrosyl ligand into the corresponding η^2-nitrito and nitrato complexes in treatment of the benzylidene dinitrosyl complex [Re{=CH(C_6H_5)}$(NO)_2$(P-^{i}Pr$_3$)$_2$][BAr^F] with dioxygen was suggested to proceed via (η^2-ON)-OO intermediate based on the DFT calculations.[72] Thus, depending on the nature of complex and reaction conditions, peroxynitrite is coordinated by the end O atom of the peroxo group or by NO. Complex **II** is unique because both these atoms are coordinated, although much weaker than in **2** (DI_{Ru-N} = 0.79; DI_{Ru-O} = 0.56 in comparison with 1.64 and 1.78, respectively, in **2**).

In the transition state TS(**II**−**III**) the Ru−O bond is strengthened (DI = 1.27) at the expense of O−O bond (DI = 0.4), whereas the Ru−NO bonding is further weakened (DI = 0.70). The resulting complex **III** could be seen as a Ru^{4+} nitrito oxo complex with large negative charges on the NO_2 and oxo ligands of −0.66 and −0.71, respectively, and DI of 0.70 and 1.47. The nitrito-group is responsible for the oxidative properties of complex **2** whereas oxo ligand is ancillary. Similar O atom transfer from nitrite to substrate was observed, for example, in cobalt nitro complexes[73] and in iron(III) porphyrin complexes.[74] The second rate-determining step is accompanied by strong weakening (DI_{Ru-N} = 0.28 in TS(**III**−**IV**)) and breaking of Ru−N bond and movement of NO group to coordinated O.

Coordination of the second CO molecule (complex **VI**) is thermodynamically much more favorable, its subsequent oxidation being kinetically more favorable than for the first molecule. This is in agreement with the experimental observation that full consumption of both oxygen atoms of one complex molecule occurs prior to reaction with the oxygen ligand of a second complex molecule. However, a mono-oxygenate does not form as an intermediate in this process, and the coordinated nitrito group again plays the role of an oxygen donor. In the resulting complex **1** NO again retains a significant negative charge of −0.38 and is doubly bound to Ru (DI = 1.86).

Although the triplet state of **2** is much higher in energy, we wanted to ensure that no intersystem crossings occur along the reaction path. All the calculated complexes with nondissociated O−O bond (in the presence and absence of coordinated CO), as well as all found transition states for O−O dissociation are significantly less stable in the triplet state. In contrast, O−O dissociation leads to complex $\mathbf{III_t}$, which is 6.1 kcal/mol more stable in the triplet than in the singlet state. This is due to the formation of $Ru^{\bullet}-O^-$ in $\mathbf{III_t}$ instead of $Ru-O^{2-}$ in **III**. CO oxidation in this complex has an internal activation barrier of 29.9 kcal/mol (vs 26.5 in the singlet state) and results in a complex $\mathbf{IV_T}$, in which NO is not directly bound to Ru, but forms an NO_2 moiety bound by an O atom. Further transformation of this complex could result in entropy-driven NO_2 dissociation, in agreement with the experimentally observed decomposition of **2** in the course of the CO oxidation reaction. NO dissociation is energetically strongly unfavorable with ΔG_{298} = 40.7 kcal/mol. Alternatively, ONO ligand transforms into NO_2 coordinated by N (complex $\mathbf{V_T}$), followed by transformation to singlet **V**, which is 1.1 kcal/mol lower in energy, and additional stabilization of the singlet state by CO coordination.

Thus, the main reaction route for oxidation of two CO molecules occurs on the singlet PES, while the triplet pathway is mainly responsible for the observed decomposition at low CO concentration. We calculated the singlet reaction path more accurately at the DLPNO-CCSD(T)/TZVP(P) level of theory (Figure 6). The results obtained generally confirm the double hybrid DFT findings.

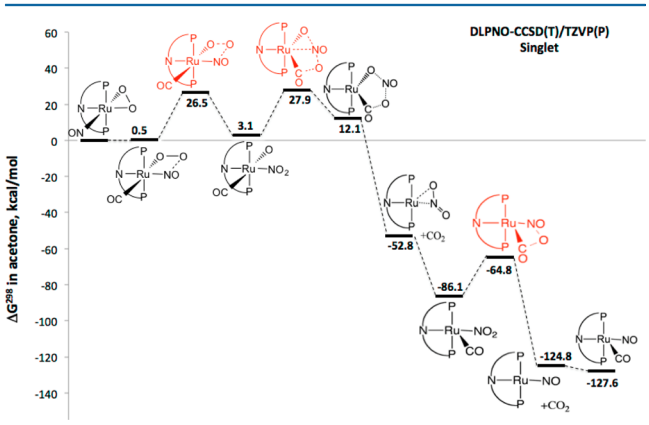

Figure 6. Reaction profiles for O−O bond dissociation in complex **2** in the singlet and triples states calculated at the DLPNO-CCSD(T)/TZVP(P) level of theory.

CONCLUSION

We have synthesized and studied two systems of $Ru^{(0)}$-$Ru^{(II)}O_2$, based on aromatic (**1**, **2**, **3**) and dearomatized (**4**, **5**, **6**) complexes. Complexes **2**, **3**, **5**, and **6** are new; complexes **2**, **5**, and **6** were also X-ray characterized. These systems activate molecular oxygen toward reaction with the mono-oxygen acceptors triphenylphosphine and CO. The nature of the intermediates involved was examined computationally, suggesting that a new type of metal−ligand cooperation because the NO ligand plays a fundamental role in those reactions (as well as possibly $Ru^{(IV)}$Oxo intermediates[75−78]). The fact that the intermediates have a low barrier for mono-oxygen transfer, and that the $Ru^{(0)}$-$Ru^{(II)}O_2$ systems can be interconverted, makes them reasonable candidates to act as intermediates in catalytic oxidation cycles.

EXPERIMENTAL SECTION

General Procedures. All experiments with metal complexes and phosphine ligands were carried out under an atmosphere of purified nitrogen in a Vacuum Atmospheres glovebox equipped with a MO 40-2 inert gas purifier or using standard Schlenk techniques. All solvents were reagent grade or better. All nondeuterated solvents were refluxed over sodium/benzophenone ketyl and distilled under argon atmosphere. Deuterated solvents were used as received. All the solvents were degassed with argon and kept in the glovebox over 4 Å molecular sieves. Commercially available reagents were used as received. ^{1}H, ^{13}C, and ^{31}P spectra were recorded at 400, 100, 162, and 376 MHz, respectively, using a Bruker AMX-300 AMX-400 NMR and AMX-500 spectrometer. All spectra were recorded at 295 K, unless otherwise noted. ^{1}H NMR and ^{13}C{^{1}H} NMR chemical shifts are reported in ppm downfield from tetramethylsilane and referenced to the residual signals of an appropriate deuterated solvent. ^{31}P NMR chemical shifts are reported in ppm downfield from H_3PO_4 and referenced to an external 85% solution of phosphoric acid in D_2O. ESI-MS spectroscopy was performed by the Department of Chemical Research Support, Weizmann Institute of Science. The nitrosyl complexes described in this work were unstable in general and specifically unstable toward light; in some cases these complexes decomposed during analysis. All reactions were performed in the dark. When accurate elemental analysis could not be obtained, HRMS was determined.

DOI: 10.1021/ic502832j
Inorg. Chem. 2015, 54, 2253−2263

Synthesis of ***2****.* A solution of **1** (10 mg, 0.0163 mmol) in 2 mL of CH_2Cl_2/C_6D_6 (1:1) in a NMR tube was bubbled with O_2 for 2 min. A color change from purple to brown took place, and complex **2** was immediately formed. The solvent was removed under a vacuum, resulting in a brown solid in quantitative yield.

Crystals of **2** suitable for X-ray analysis (with BAr^F anion) were obtained by fast (3−4 min) partial evaporation of an ethereal solution of freshly prepared **2**. Because of the instability of **2**, the crystals were *immediately* placed in Paratone oil and flash frozen in a nitrogen stream at 100 K. Data were collected *immediately*.

$^{31}P\{^1H\}$ NMR (121 MHz, CD_2Cl_2, C_6D_6): 67.21 (s). ^1H NMR (300 MHz, CD_2Cl_2, C_6D_6): 7.72 (t, 1H, J_{HH} = 7.4 Hz, Py-H4), 7.51 (d, J_{HH} = 7.4 Hz, 2H, Py-H3, H5),), 3.74 (m, 2H, PC*H*HPy), 3.44 (m, 2H, PC*H*HPy), 1.07 (m, 36H, $PC(CH_3)_3$).

$^1H\{^{31}P\}$ NMR (300 MHz, CD_2Cl_2, C_6D_6): 7.71 (t, 1H, J_{HH} =7.4 Hz, Py-H4), 7.51 (d, J_{HH} = 7.4 Hz, 2H, Py-H3, H5),), 3.77 (d, 2H, J_{HH} =17.1 Hz PC*H*HPy), 3.45 (d, 2H, J_{HH} =17.1 Hz PC*H*HPy), 1.07 (s, 18H, $PC(CH_3)_3$), 1.05 (s, 18H, $PC(CH_3)_3$).

$^{13}C\{^1H\}$ NMR (CD_2Cl_2, C_6D_6): 164.7 (s, Py-C2, C6), 143.4 (s, Py-C4), 124 (s, Py-C3, C5), 39.1 (t, J_{CP} = 6 Hz, $PC(CH_3)_3$), 38.8 (t, J_{CP} = 6 Hz, $PC(CH_3)_3$), 36.2 (t, J_{CP} = 7.8 Hz, PCH_2Py), 29.9 (bm, $PC(CH_3)_3$), 29.4 (bm, $PC(CH_3)_3$).

IR: ν N−O 1646.3 cm^{-1}, ν O−O 796.4 cm^{-1}, ν $^{18}O-^{18}O$ 759.6 cm^{-1}.

HRMS: *m*/*z* 599.1816 (M+, calcd *m*/*z* 599.1792).

Anal. Calcd for $C_{23}H_{43}BF_4N_2O_3PRu$: C, 42.8; H, 6.7; N, 4.3. Found: C, 42.1; H, 6.8; N, 4.2.

Synthesis of ***3*** *from* ***1****.* To a solution of complex **1** (18 mg, 0.029 mmol) in 1 mL of acetone was added 2 equiv (1.43 mL) of CO gas in a septum screw cap NMR tube, and the mixture was shaken at room temperature. There was immediate color change and the solvent was removed under vacuum, leaving pure **3** in quantitative yield.

$^{31}P\{^1H\}$ NMR (121 MHz, acetone-d_6): 82.00 (s). ^1H NMR (300 MHz, acetone-d_6): 8.20 (t, 1H, J_{HH} = 7.8 Hz, Py-H4), 7.97 (d, 2H, J_{HH} = 7.8 Hz, Py-H3, H3), 4.44 (m, 2H, PC*H*HPy), 4.28 (m, 2H, PCH*H*Py), 1.28 (m, 36H, $PC(CH_3)_3$).

$^{13}C\{^1H\}$ NMR (125 MHz, acetone-d_6): 191.7 (m, *C*O) 164.8 (s, Py-C2), 142.2 (s, Py-C4), 123.8 (s, Py-C3), 46.5 (bs, PCH_2Py), 38.1 (bm, $PC(CH_3)_3$), 37.2 (m, $PC(CH_3)_3$), 30.0 (bs, $PC(CH_3)_3$), 28.8 (bm, $PC(CH_3)_3$).

IR: ν N−O 1572 cm^{-1}, ν C−O 1940 cm^{-1}.

HRMS: *m*/*z* 555.1857 (M+, calcd *m*/*z* 555.1843).

Synthesis of ***5****.* A C_6D_6 (1 mL) solution of **4** (10 mg, 0.019 mmol) in a NMR tube was bubbled with O_2 for 30 s. An immediate color change from purple to brown was observed. The solvent was removed under a vacuum, yielding **5** as a brown solid in quantitative yield.

Single crystals of **5** suitable for X-ray diffraction were obtained by slow evaporation of an ethereal solution of **5**.

$^{31}P\{^1H\}$ NMR (121.1 MHz, C_6D_6): 86.83 (d, J_{PP} = 344 Hz, 1P), 45.21 (d, J_{PP} = 344 Hz, 1P). ^1H NMR (C_6D_6): 6.43 (m, 1H, Py-H4), 6.30 (d, J_{HH} = 8.7 Hz, 1H, Py-H3), 5.36 (d, J_{HH} = 6.3 Hz, 1H, Py-H5), 3.54 (d, J_{HP} = 6.3 Hz, 1H, PC*H*Py), 2.85 (dd, J_{HH} = 15.3 Hz, J_{HP} =10.5 Hz,, 1H, PC*H*HPy), 2.49 (dd, J_{HH} = 13.5 Hz, J_{HP} =10.5 Hz, 1H, PCH*H*Py), 1.50 (d, J_{HP} = 13.5 Hz, 9H, $PC(CH_3)_3$), 1.32 (d, J_{HP} = 13.5 Hz, 9H, $PC(CH_3)_3$), 1.23 (d, J_{HP} = 13.2 Hz, 9H, $PC(CH_3)_3$), 1.03 (d, J_{HP} = 13.2 Hz, 9H, $PC(CH_3)_3$).

$^1H\{^{31}P\}$ NMR (300.1 MHz, C_6D_6): 6.40 (dd, J_{HH} = 9 Hz, J_{HH} = 6.3 Hz, 1H, Py-H4), 6.30 (d, J_{HH} = 9 Hz, 1H, Py-H3), 5.36 (d, J_{HH} = 6 Hz, 1H, Py-H5), 3.54 (1H, PC*H*Py), 2.85 (dd, J_{HH} = 15.6 Hz, Hz,, 1H, PC*H*HPy), 2.48 (d, J_{HH} = 15.6 Hz, 1H, PCH*H*Py), 1.50 (s, 9H, $PC(CH_3)_3$), 1.32 (s, J_{HP} = 13.5 Hz, 9H, $PC(CH_3)_3$), 1.23 (s, 9H, $PC(CH_3)_3$), 1.03 (s, 9H, $PC(CH_3)_3$).

$^{13}C\{^1H\}$ NMR (100 MHz, C_6D_6): 172.3 (dd, J_{CP} = 13.4 Hz, J_{CP} = 3 Hz, Py-C2), 167.5 (s, Py-C6), 132.2 (s, Py-C4), 116.3 (d, J_{CP} = 16.1 Hz, Py-C3), 100.2 (d, J_{CP} = 9 Hz, Py-C5), 68.1 (d, J_{CP} = 52.3 Hz, P*C*HPy), 34.5 (dd, J_{CP} = 17 Hz, J_{CP} = 2.3 Hz, PCH_2Py), 30.7 (m, $PC(CH_3)_3$), 29.8 (m, $PC(CH_3)_3$), 29.7 (t, J_{CP} = 6 Hz, $PC(CH_3)_3$), 29.1 (m, $PC(CH_3)_3$).

IR: ν N−O 1733.0 cm^{-1}, ν O−O 1020.6 cm^{-1}.

HRMS: *m*/*z* 559.1824 (MH+, calcd *m*/*z* 559.1792).

Synthesis of ***6****.* To a solution of complex **4** (20 mg, 0.038 mmol) in 1 mL of C_6D_6 was added 1 equiv (0.93 mL) of CO in a septum-screw cap NMR tube, and the mixture was shaken at room temperature. There was an immediate color change from purple to red, and the solvent was removed under a vacuum, quantitatively yielding pure **6**, as analyzed by $^{31}P\{^1H\}$ NMR.

Single crystals suitable for X-ray diffraction were obtained by cooling a toluene solution of **6** to −70 °C for a few hours.

$^{31}P\{^1H\}$ NMR (6-^{13}CO, 162 MHz, C_6D_6): 82.68 (dd, J_{PP} = 154.0 Hz, J_{PC} = 12.0 Hz, 1P), 81.18 (dd, J_{PP} = 154.0 Hz, J_{PC} = 12.0 Hz, 1P).

^1H NMR (6-^{13}CO, 300.1 MHz, C_6D_6): 6.61 (m, 1H, Py-H4), 6.57 (d, J_{HH} = 8.0 Hz, 1H, Py-H3), 5.36 (d, J_{HH} = 6.0 Hz, 1H, Py-H5), 3.61 (d, J_{HP} = 3.0 Hz, 1H, PC*H*Py), 2.99 (dd, J_{HH} = 16.4 Hz, J_{HP} = 6.0 Hz, 1H, PC*H*HPy), 2.81 (dd, J_{HH} = 16.4 Hz, J_{HP} = 10.8 Hz, 1H, PCH*H*Py), 1.21 (m, 18H, $PC(CH_3)_3$), 0.89 (m, 18H, $PC(CH_3)_3$.

$^1H\{^{31}P\}$ NMR (6-^{13}CO, 300.1 MHz, C_6D_6): 6.63 (m, 1H, Py-H4), 6.58 (d, J_{HH} = 8.0 Hz, 1H, Py-H3), 5.62 (d, J_{HH} = 6.3 Hz, 1H, Py-H5), 3.61 (s, 1H, PC*H*Py), 2.99 (d, J_{HH} = 16 Hz, 1H, PC*H*HPy), 2.80 (dd, J_{HH} = 16 Hz, 1H, PCH*H*Py), 1.21 (d, 18H, J_{HC} = 3.8 Hz, $PC(CH_3)_3$), 0.90 (m, 18H, J_{HC} = 11.7 Hz, $PC(CH_3)_3$.

$^{13}C\{^1H\}$ NMR (6-^{13}CO, 100 MHz, C_6D_6): 208.5 (bs, ^{13}CO) 172.1 (s, Py-C2), 158.2 (s, Py-C6), 132.5 (s, Py-C4), 114.6 (dd, J_{CP} = 14.1 Hz, J_{CC} = 2.2 Hz, Py-C3), 99.4 (d, J_{CP} = 9.5 Hz, Py-C5), 62.4 (dd, J_{CP} = 46.6 Hz, J_{CC} = 6.5 Hz, PCHPy), 36.9 (m, PCH_2Py), 36.8 (m, $PC(CH_3)_3$), 36.0 (m, $PC(CH_3)_3$), 29.7 (d, J_{CP} = 4.7 Hz, $PC(CH_3)_3$), 29.4 (d, J_{CP} = 4.0 Hz, $PC(CH_3)_3$), 29.2 (d, J_{CP} = 2.4 Hz, $PC(CH_3)_3$), 28.4 (d, J_{CP} = 2.7 Hz, $PC(CH_3)_3$).

IR: ν N−O 1558 cm^{-1}, ν C−O 1941 cm^{-1}.

MS: *m*/*z* 555.05 (MH+, calcd *m*/*z* 555.18).

HRMS: *m*/*z* 555.1844 (MH+, calcd *m*/*z* 555.1843).

Reaction of ***5*** *with MeI.* To a solution of **5** (16.7 mg, 0.03 mmol) in 1 mL of C_6D_6 was added one drop of MeI in a J. Young NMR tube. The mixture was placed in a 60 °C oil bath for 1.5 h to give the oxidized ligand as the only product according to NMR analysis.

*General Procedure for Reactions of Ru(O_2) Complexes (****2*** *and* ***5****) with Phosphines.* To a solution of the specified Ru(O_2) complexes (**2** or **5**, 0.03 mmol) in 1.5 mL of the specified solvent (acetone or C_6D_6) was added 1 equiv of the specified phosphine, and the mixture was stirred for the specified time (1 s to 3 days) and then transferred to an NMR tube, and the products were determined by NMR analysis.

Reaction of ***2*** *with PEt_3.* To a solution containing 2 equiv of **2** (19.4 mg, 0.03 mmol) in 1.5 mL of acetone were added 2 equiv of PEt_3 (3.5 mg, 0.03 mmol), and the solution was stirred for a few seconds. The solution was then transferred to an NMR tube, and ^{31}P NMR analysis showed the formation of 1 equiv of **1** (50% yield), 1 equiv (50% yield) of **2**, and 2 equiv of triethylphosphine oxide (100% yield).

Reaction of ***2*** *with PPh_3.* To a solution containing 2 equiv of **2** (19.4 mg, 0.03 mmol) in 1.5 mL of acetone were added 2 equiv of PPh_3 (7.7 mg, 0.03 mmol), and the mixture was stirred for a few seconds. The solution was then transferred to an NMR tube, and ^{31}P NMR and ^1H NMR analysis of revealed the formation of 1 equiv of **1** (50% yield), 1 equiv of **2** (50% yield), and 2 equiv of triphenylphosphine oxide (100% yield).

Reaction of ***5*** *with PPh_3 in Acetone.* To a solution containing 2 equiv of **5** (16.7 mg, 0.03 mmol) in 1.5 mL of acetone were added 2 equiv of PPh_3 (7.7 mg, 0.03 mmol), and the solution was stirred for a few seconds. The solution was then transferred to an NMR tube and ^{31}P NMR analysis revealed the formation of 1 equiv of **4** (50% yield), 1 equiv of **5** (50% yield), and 2 equiv of triphenylphosphine oxide (100% yield).

Reaction of ***5*** *with PPh_3 in C_6D_6.* To a solution of 2 equiv of **5** (16.7 mg, 0.03 mmol) in 1.5 mL of C_6D_6 were added 2 equiv of PPh_3 (7.7 mg, 0.03 mmol), and the mixture was stirred for a few seconds. The reaction mixture was then transferred to an NMR tube, and ^{31}P NMR and ^1H NMR analysis of it revealed the formation of 1 equiv of **4** (50% yield), 1 equiv of **5** (50% yield), and 2 equiv of triphenylphosphine oxide (100% yield).

Reaction of ***5*** *with $^tBu_3P$ in C_6D_6.* To a solution of 2 equiv of **5** (16.7 mg, 0.03 mmol) in 1.5 mL of acetone were added 2 equiv of

DOI: 10.1021/ic502832j
Inorg. Chem. 2015, 54, 2253−2263

$^{t}Bu_3P$ (6.1 mg, 0.03 mmol), and the solution was stirred for 3 days. It was then transferred to an NMR tube and ^{31}P NMR analysis of it revealed the formation of 1 equiv of **4** (50% yield), 1 equiv of **5** (50% yield), and in addition two unidentified compounds, which exhibit singlet peaks.

*Reaction of **2** with One Equivalent of CO.* To a solution of **2** (19.4 mg, 0.03 mmol) in 0.8 mL of acetone in a septum-screw cap NMR tube was added 1 equiv of CO (0.73 mL) gas at room temperature. The mixture was shaken and ^{31}P NMR analysis after 1 h, 2 h, and overnight showed only formation of decomposition products.

*Reaction of **2** with Three Equivalents of CO.* To a solution of **2** (19.4 mg, 0.03 mmol) in 0.8 mL of acetone in a septum-screw cap NMR tube was added 3 equiv of CO (2.20 mL) gas at room temperature. The solution was shaken and ^{31}P NMR analysis taken after 1 h, 2 h, and overnight showed formation of an unseparable mixture of products that converge to give **3** as the only product in quantitative yield after a night at room temperature. The structure of **3** was verified by ^{1}H NMR and ^{13}C NMR spectroscopy.

*Reactions of **5** with One Equivalent of CO.* To a solution of **5** (16.7 mg, 0.03 mmol) in 0.8 mL of C_6D_6 in a septum-screw cap NMR tube was added 1 equiv of CO (0.73 mL) gas at room temperature. The solution was shaken and ^{31}P NMR analysis taken after 1 h, 2 h, and overnight showed only the formation of decomposition products.

*Reaction of **5** with Three Equivalents of CO.* To a solution of **5** (16.7 mg, 0.03 mmol) in 0.8 mL of C_6D_6 in a septum-screw cap NMR tube were added 3 equivalents of CO (2.20 mL) gas at room temperature. The solution was shaken and ^{31}P NMR analysis after 1 h, 2 h, and overnight showed that an unseparable mixture of products was formed that converge to give complex **6** as the only product in quantitative yield after a night at room temperature. The structure of **6** was verified by ^{1}H NMR and ^{13}C NMR spectroscopy.

*General Procedure for Reactions of **1** with Dioxirane.* To a solution of **1** in 1.5 mL of acetone at the specified temperature was added 1 equiv of freshly degassed and titrated dioxirane (0.1−0.075M, 0.03 mmol) in 1.5 mL of acetone, and the mixture was stirred or shaken for the specified time (rt: 10 min; −34 °C: 30 min; −78 °C 16 h), and the products were analyzed by NMR.

X-ray Crystal Structure Determination of Complexes. Crystal data were measured at 100 K on a Bruker Apex-II KappaCCD diffractometer equipped with [λ(Mo−Kα) = 0.71073 Å] radiation, graphite monochromator and MiraCol optics. The data were processed with APEX-II collect package programs. Structures were solved by the AUTOSTRUCTURE module and refined with full-matrix least-squares refinement based on F^2 with SHELXL-97. Full details can be found in the CIF files and Table 4S in the Supporting Information.

COMPUTATIONAL METHODS

The geometries of the molecules were optimized using the PBE0 hybrid density functional,[79] in conjunction with the PC-1 basis set. This basis set is a combination of Jensen's polarization consistent pc-1 basis set[80] for the main group elements and the relativistic energy-consistent pseudopotential (RECP) and associated basis set SDD[81] for ruthenium, with an added f-type polarization exponent taken as the geometric average of the two f-exponents given by Martin and Sundermann.[82] This combination is of double-ζ plus polarization quality. For comparison, several important complexes were optimized at the same level of theory with acetone as solvent, as well as in the gas phase at the PBE0/def2-TZVP-D3BJ level, that is, using the larger Weigend-Ahlrichs[83] triple-ζ plus polarization basis set def2-TZVP as well as Grimme's empirical dispersion correction[84] using the Becke-Johnson damping function.[85] (The Weigend-Ahlrichs basis sets employ the same RECP as SDD for elements heavier than Kr: for lighter elements they are all-electron.) In both cases the optimized geometries were very similar to the PBE0/PC1 results: a comparison of the geometries obtained for complex 2 can be found in Table 1S in the Supporting Information. All PBE0 calculations were carried out using the Gaussian 09 software package.[86]

All structures were fully optimized in the gas phase and characterized as minima or transition states by calculating the harmonic vibrational frequencies. The connectivity of the transition states was confirmed by performing intrinsic reaction coordinate (IRC) calculations[87] with 10 points in each direction followed by full optimization of the resulting geometries. Bulk solvent effects of the experimental acetone or dichloromethane (DCM) media have been taken into account via the self-consistent reaction field (SCRF) method, using the integral equation formalism polarizable continuum model (PCM)[88] as implemented in Gaussian 09.

In order to improve the accuracy of the calculated energetics (particularly the barrier heights) we carried out single-point energy calculations using the DSD-PBEB95-D3BJ[89] and DSD-PBEP86-D3BJ[90] double-hybrid functionals. DSD-PBEP86 was shown[89,90] to yield thermochemistry and barrier heights comparable to composite ab initio methods, while DSD-PBEB95-D3BJ additionally yielded accurate singlet−triplet splittings (see Table 12 in ref 89). In the double-hybrid calculations we employed the def2-TZVP(P) basis set, which refers to def2-TZVP on the main group elements and def2-TZVPP on the transition metal. In practice, the difference amount to 2f1g rather than 1f polarization functions on the metal. This particular set of calculations was carried out using ORCA[91] version 3.0.2: the RI (resolution of the identity) approximation[92] as implemented in ORCA was employed, using the def2-TZVP/JK auxiliary basis set[93] for the Coulomb and exchange integrals, and the def2-TZVP/C auxiliary basis sets[94] for the RI-MP2-like part. Especially the latter affords a dramatic reduction in both CPU time and I/O overhead.

Unless stated otherwise, energetic data presented in the main text of the paper are based on the resulting DSD-PBEB95-D3BJ energies with solvation and statistical thermodynamic effects obtained at the PBE0/pc-1 level in acetone at 298.15 K. A modified rigid rotor-harmonic oscillator (RRHO) correction was applied. The corresponding data obtained in the DSD-PBEP86 calculations could be found in Supporting Information.

As an additional sanity check, we repeated our single-point energy calculations for the singlet surface only using the DLPNO-CCSD(T) (domain localized pair natural orbital−coupled cluster with all single and double substitutions plus quasiperturbative triple excitations) method of Neese and co-workers[95] as implemented in ORCA. The same orbital and auxiliary basis sets, as well as the same RECP, as for the double hybrid calculations were employed. Two sets of calculations were carried out, one with the various cutoff parameters left at their default values TCutPNO = 3.331×10^{-7}; TCutPairs = 1×10^{-4}; TCutMKN = 1×10^{-3}; TCutTNO = 1×10^{-7}, the other with TCutPairs tightened to 1×10^{-5}.

For qualitative interpretation of the computational results, the PBE0/PC1 electron density of the complexes in optimized geometries was analyzed using natural bond orbital (NBO).[96] Full topological analysis was performed using the program AIMALL.[97]

ASSOCIATED CONTENT

Supporting Information

Copies of NMR spectra of the new complexes, and CIF files giving X-ray data for complexes **2**, **5**, and **6** are included. This material is available free of charge via the Internet at http://pubs.acs.org.

AUTHOR INFORMATION

Corresponding Authors

*(D.M.) E-mail: david.milstein@weizmann.ac.il. Fax: +972-89343039.

*(J.M.L.M.) E-mail: gershom@weizmann.ac.il.

Notes

The authors declare no competing financial interest.

DOI: 10.1021/ic502832j
Inorg. Chem. 2015, 54, 2253−2263

■ ACKNOWLEDGMENTS

This research was supported by the European Research Council under the FP7 framework (ERC No. 246837), the Israel Science Foundation, and the MINERVA Foundation. We thank Dr. Haim Weissman, Prof. Ronny Neumann, and Dr. Delina Barats Damatov for valuable discussions. D.M. is the holder of the Israel Matz Professorial Chair of Organic Chemistry.

■ REFERENCES

(1) (a) Wilke, G.; Schott, H.; Heimbach, P. *Angew. Chem., Int. Ed.* **1967**, *6*, 92−93. (b) Holland, P. L. *Dalton Trans.* **2010**, *39*, 5415−5425. (c) Boisvert, L.; Goldberg, G. *Acc. Chem. Res.* **2012**, *45*, 899−910.
(2) Graham, B. W.; Laing, K. R.; O'Connor, C. J.; Roper, W. R. *J. Chem. Soc., Dalton Trans.* **1972**, *0*, 1237−1243.
(3) Morales-Morales, D. R.; R. Roger, E. C. *Inorg. Chim. Acta* **2001**, *321*, 181−184.
(4) Ogasawara, M.; Macgregor, S. A.; Streib, W. E.; Folting, K.; Eisenstein, O.; Caulton, K. G. *J. Am. Chem. Soc.* **1996**, *118*, 10189−10199.
(5) Shen, J.; Stevens, E. D.; Nolan, S. P. *Organometallics* **1998**, *17*, 3875−3882.
(6) Yoshinari, A.; Tazawa, A.; Kuwata, S.; Ikariya, T. *Chem.—Asian J.* **2012**, *7*, 1417−1425.
(7) Frech, C. M.; Shimon, L. J. W.; Milstein, D. *Helv. Chim. Acta* **2006**, *89*, 1730−1739.
(8) Vigalok, A.; Shimon, L. J. W.; Milstein, D. *Chem. Commun.* **1996**, 1673−1674.
(9) Poverenov, E.; Efremenko, I.; Frenkel, A. I.; Ben-David, Y.; Shimon, L. J. W.; Leitus, G.; Konstantinovski, L.; Martin, J. M. L.; Milstein, D. *Nature* **2008**, *455*, 1093−1096.
(10) Que, L.; Tolman, W. B. *Nature* **2008**, *455*, 333−340 and references therein.
(11) Moro-oka, Y.; Akita, M. *Catal. Today* **1998**, *41*, 327−338.
(12) Mimoun, H. *Angew. Chem., Int. Ed.* **1982**, *21*, 734−750.
(13) Akita, M.; Moro-oka, Y. *Catal. Today* **1998**, *44*, 183−188.
(14) Murahashi, S.-I. *Angew. Chem., Int. Ed.* **1995**, *34*, 2443−2465.
(15) Strukul, G. *Angew. Chem., Int. Ed.* **1998**, *37*, 1198−1209.
(16) Meier, G.; Braun, T. *Angew. Chem.* **2012**, *124*, 12732−12737.
(17) Campos-Martin, J. M.; Blanco-Brieva, G.; Fierro, J. L. G. *Angew. Chem., Int. Ed.* **2006**, *45*, 6962−6984 and references therein.
(18) Green, M. T.; Dawson, J. H.; Gray, H. B. *Science* **2004**, *304*, 1653−1656.
(19) Rohde, J. U. *Science* **2003**, *299*, 1037−1039.
(20) Yoshizawa, K. *Acc. Chem. Res.* **2006**, *39*, 375−382.
(21) Meunier, B. *Biomimetic Oxidations Catalyzed by Transition Metal Complexes*; Macmillan Publishers Limited: New York, 2000.
(22) Sheldon, R. A.; Kochi, J. K. *Metal-Catalyzed Oxidations of Organic Compounds*; Macmillan Publishers Limited: New York, 1981.
(23) Holm, R. H. *Chem. Rev.* **1987**, *87*, 1401−1449.
(24) Nugent, W. A.; Mayer, J. M. *Metal-Ligand Multiple Bonds*; Macmillan Publishers Limited: New York, 1988.
(25) Neumann, R.; Dahan, M. 1997, *388*, 353−355.
(26) Jones, R.; Jayaraj, K.; Gold, A.; Kirk, M. L. *Inorg. Chem.* **1998**, *37*, 2842−2843.
(27) Inscore, F. E.; McNaughton, R.; Westcott, B. L.; Helton, M. E.; Jones, R.; Dhawan, I. K.; Enemark, J. H.; Kirk, M. L. *Inorg. Chem.* **1999**, *38*, 1401−1410.
(28) Carducci, M. D.; Brown, C.; Solomon, E. I.; Enemark, J. H. *J. Am. Chem. Soc.* **1994**, *116*, 11856−11868.
(29) Parkin, G. *Terminal Chalcogenido Complexes of the Transition Metals*; John Wiley & Sons, Inc.: New York, 2007.
(30) MacBeth, C. E.; Golombek, A. P.; Young, V. G.; Yang, C.; Kuczera, K.; Hendrich, M. P.; Borovik, A. S. *Science* **2000**, *289*, 938−941.
(31) O'Halloran, K. P.; Zhao, C.; Ando, N. S.; Schultz, A. J.; Koetzle, T. F.; Piccoli, P. M. B.; Hedman, B.; Hodgson, K. O.; Bobyr, E.; Kirk, M. L.; Knottenbelt, S.; Depperman, E. C.; Stein, B.; Anderson, T. M.; Cao, R.; Geletii, Y. V.; Hardcastle, K. I.; Musaev, D. G.; Neiwert, W. A.; Fang, X.; Morokuma, K.; Wu, S.; Kögerler, P.; Hill, C. L. *Inorg. Chem.* **2012**, *51*, 7025−7031.
(32) (a) Gnanaprakasam, B.; Balaraman, E.; Ben-David, Y.; Milstein, D. *Angew. Chem.* **2011**, *123*, 12448−12452. (b) Gnanaprakasam, B.; Balaraman, E.; Ben-David, Y.; Milstein, D. *Angew. Chem., Int. Ed.* **2011**, *50*, 12240−12244.
(33) Zhang, J.; Gandelman, M.; Shimon, L. J. W.; Rozenberg, H.; Milstein, D. *Organometallics* **2004**, *23*, 4026−4033.
(34) Zhang, J.; Leitus, G.; Ben-David, Y.; Milstein, D. *J. Am. Chem. Soc.* **2005**, *127*, 10840−10841.
(35) Zhang, J.; Gandelman, M.; Shimon, L. J. W.; Milstein, D. *Dalton Trans.* **2007**, 107−113.
(36) Gargir, M.; Ben-David, Y.; Leitus, G.; Diskin-Posner, Y.; Shimon, L. J. W.; Milstein, D. *Organometallics* **2012**, *31*, 6207−6214.
(37) Fogler, E.; Balaraman, E.; Ben-David, Y.; Leitus, G.; Shimon, L. J. W.; Milstein, D. *Organometallics* **2011**, *30*, 3826−3833 and references therein.
(38) Zhang, J.; Leitus, G.; Ben-David, Y.; Milstein, D. *Angew. Chem., Int. Ed.* **2006**, *45*, 1113−1115.
(39) Balaraman, E.; Fogler, E.; Milstein, D. *Chem. Commun.* **2012**, *48*, 1111−1113.
(40) Gunanathan, C.; Milstein, D. *Angew. Chem., Int. Ed.* **2008**, *47*, 8661−8664.
(41) Gnanaprakasam, B.; Zhang, J.; Milstein, D. *Angew. Chem., Int. Ed.* **2010**, *49*, 1468−1471.
(42) Srimani, D.; Feller, M.; Ben-David, Y.; Milstein, D. *Chem. Commun.* **2012**, *48*, 11853−11855.
(43) Gunanathan, C.; Shimon, L. J. W.; Milstein, D. *J. Am. Chem. Soc.* **2009**, *131*, 3146−3147.
(44) Kossoy, E.; Diskin-Posner, Y.; Leitus, G.; Milstein, D. *Adv. Synth. Catal.* **2012**, *354*, 497−504.
(45) van der Boom, M. E.; Milstein, D. *Chem. Rev.* **2003**, *103*, 1759−1792 and references therein.
(46) Gnanaprakasam, B.; Ben-David, Y.; Milstein, D. *Adv. Synth. Catal.* **2010**, *352*, 3169−3173.
(47) (a) Balaraman, E.; Ben-David, Y.; Milstein, D. *Angew. Chem.* **2011**, *123*, 11906−11909. (b) Balaraman, E.; Ben-David, Y.; Milstein, D. *Angew. Chem., Int. Ed.* **2011**, *50*, 11702−11705.
(48) Balaraman, E.; Gunanathan, C.; Zhang, J.; Shimon, L. J. W.; Milstein, D. *Nat. Chem.* **2011**, *3*, 609−614.
(49) Gnanaprakasam, B.; Milstein, D. *J. Am. Chem. Soc.* **2011**, *133*, 1682−1685.
(50) Balaraman, E.; Gnanaprakasam, B.; Shimon, L. J. W.; Milstein, D. *J. Am. Chem. Soc.* **2010**, *132*, 16756−16758.
(51) Fogler, E.; Iron, M. A.; Zhang, J.; Ben-David, Y.; Diskin−Posner, Y.; Leitus, G.; Shimon, L. J. W.; Milstein, D. *Inorg. Chem.* **2013**, *52*, 11469−11479 and references therein.
(52) (a) Zhang, J.; Balaraman, E.; Leitus, G.; Milstein, D. *Organometallics* **2011**, *30*, 5716−5724.
(53) Ben-Ari, E.; Leitus, G.; Shimon, L. J. W.; Milstein, D. *J. Am. Chem. Soc.* **2006**, *128*, 15390−15391.
(54) Iron, M. A.; Ben-Ari, E.; Cohen, R.; Milstein, D. *Dalton Trans.* **2009**, *s.v.*, 9433−9439 Intentional?.
(55) Gunanathan, C.; Ben-David, Y.; Milstein, D. *Science* **2007**, *317*, 790−792.
(56) Gunanathan, C.; Milstein, D. In *Bifunctional Molecular Catalysis*; Ikariya, T., Shibasaki, M., Eds.; Springer: Berlin Heidelberg, 2011; Vol. *37*, p 55−84 and references therein.
(57) Langer, R.; Diskin-Posner, Y.; Leitus, G.; Shimon, L. J. W.; Ben-David, Y.; Milstein, D. *Angew. Chem., Int. Ed.* **2011**, *50*, 9948−9952.
(58) Langer, R.; Leitus, G.; Ben-David, Y.; Milstein, D. *Angew. Chem.* **2011**, *123*, 2168−2172.
(59) Montag, M.; Efremenko, I.; Diskin-Posner, Y.; Ben-David, Y.; Martin, J. M. L.; Milstein, D. *Organometallics* **2011**, *31*, 505−512.
(60) Vogt, M.; Gargir, M.; Iron, M. A.; Diskin-Posner, Y.; Ben-David, Y.; Milstein, D. *Chemistry − A European Journal* **2012**, *18*, 9194−9197.
(61) Gunanathan, C.; Milstein, D. *Science* **2013**, 341.

DOI: 10.1021/ic502832j
Inorg. Chem. 2015, 54, 2253−2263

(62) Valentine, J. S. *Chem. Rev.* **1973**, *73*, 235−245 and references therein.
(63) Ogasawara, M.; Huang, D.; Streib, W. E.; Huffman, J. C.; Gallego-Planas, N.; Maseras, F.; Eisenstein, O.; Caulton, K. G. *J. Am. Chem. Soc.* **1997**, *119*, 8642−8651.
(64) In the gas phase, excitation of O_2 into the lowest singlet state, $O_2(X^3\Sigma_g^-) \rightarrow O_2(a^1\Delta_g)$ is endothermic by 22.5 kcal/mol: Schweitzer, C.; Schmidt, R. *Chem. Rev.* **2003**, *103*, 1685−1757. See also Huber, K. P.; Herzberg, G. *Constants of Diatomic Molecules*; Van Nostrand Reinhold, New York, 1979.
(65) See Figure 1 for notation.
(66) Both reaction profiles shown in Supporting Information have slightly lower apparent activation energies at the DSD-PBEB95/TZVP(P) level of theory. For the singlet PES transition states shown in Figure 5 are found to be energetically preferred in the DLPNO-CCSD(T) calculations. The presented reaction profile in the triplet state is not the lowest energy pathway since TS for O-O dissociation in complex **2** in absence of CO is 3.4 kcal/mol lower in energy. Similar results were obtained at the DSD-PBEP86/TZVP(P) level, see Supporting Information.
(67) (a) Sumimoto, M.; Iwane, N.; Takahama, T.; Sakaki, S. *J. Am. Chem. Soc.* **2004**, *126*, 10457−10471. (b) Braga, A. A. C.; Ujaque, G.; Maseras, F. *Organometallics* **2006**, *25*, 3647−3658.
(68) Sakaki, S.; Takayama, T.; Sumimoto, M.; Sugimoto, M. *J. Am. Chem. Soc.* **2004**, *126*, 3332.
(69) Gadzhiev, O. B.; Ignatov, S. K.; Gangopadhyay, S.; Masunov, A. E.; Petrov, A. I. *J. Chem. Theory Comput.* **2011**, *7*, 2021−2024.
(70) Kurtikyan, T. S.; Eksuzyan, Sh. R.; Hayrapetyan, V. A.; Martirosyan, G. G.; Hovhannisyan, G. S.; Goodwin, J. A. *J. Am. Chem. Soc.* **2012**, *134*, 13861−13870.
(71) Park, G. Y.; Deepalatha, S.; Puiu, S. C.; Lee, D.-H.; Mondal, B.; Sarjeant, A. A. N.; del Rio, D.; Pau, M. Y. M.; Solomon, E. I.; Karlin, K. D. *J. Biol. Inorg. Chem.* **2009**, *14*, 1301−1311.
(72) Frech, C. M.; Blacque, O.; Schmalle, H. W.; Berke, H. *Dalton Trans.* **2006**, 4590−4598.
(73) Tovrog, B. S.; Mares, F.; Diamond, S. E. *J. Am. Chem. Soc.* **1980**, *102*, 6616−6618.
(74) (a) Khin, C.; Heinecke, J.; Ford, P. C. *J. Am. Chem. Soc.* **2008**, *130*, 13830−13831. (b) Afshar, R. K.; Eroy-Reveles, A. A.; Olmstead, M. M.; Mascharak, P. K. *Inorg. Chem.* **2006**, *45*, 10347.
(75) Sala, X.; Romero, I.; Rodríguez, M.; Escriche, L.; Llobet, A. *Angew. Chem., Int. Ed.* **2009**, *48*, 2842−2852 and references therein..
(76) Romero, I.; Rodríguez, M.; Sens, C.; Mola, J.; Rao Kollipara, M.; Francàs, L.; Mas-Marza, E.; Escriche, L.; Llobet, A. *Inorg. Chem.* **2008**, *47*, 1824−1834 and references within.
(77) Meyer, T. J.; Huynh, M. H. V. *Inorg. Chem.* **2003**, *42*, 8140−8160.
(78) Llobet, A. *Inorg. Chim. Acta* **1994**, *221*, 125−131.
(79) Adamo, C.; Cossi, M.; Barone, V. *J. Mol. Struct. (THEOCHEM)* **1999**, *493*, 145−157.
(80) (a) Jensen, F. *J. Chem. Phys.* **2001**, *115*, 9113−9125. (b) Jensen, F. *J. Chem. Phys.* **2002**, *116*, 7372−7379.
(81) Dolg, M. In *Modern Methods and Algorithms of Quantum Chemistry*; Grotendorst, J., Ed.; Jülich, 2000; Vol. *1*, pp 479−508.
(82) Martin, J. M. L.; Sundermann, A. *J. Chem. Phys.* **2001**, *114*, 3408−3420.
(83) Weigend, F.; Ahlrichs, R. *Phys. Chem. Chem. Phys.* **2005**, *7*, 3297−3305.
(84) (a) Grimme, S.; Antony, J.; Ehrlich, S.; Krieg, H. *J. Chem. Phys.* **2010**, *132*, 154104. (b) Grimme, S.; Ehrlich, S.; Goerigk, L. *J. Comput. Chem.* **2011**, *32*, 1456−1465.
(85) (a) Becke, A. D.; Johnson, E. R. *J. Chem. Phys.* **2005**, *122*, 154101. (b) Johnson, E. R.; Becke, A. D. *J. Chem. Phys.* **2005**, *123*, 024101. (c) Johnson, E. R.; Becke, A. D. *J. Chem. Phys.* **2006**, *124*, 174104.
(86) Frisch, M. J.; Trucks, G. W.; Schlegel, H. B.; Scuseria, G. E.; Robb, M. A.; Cheeseman, J. R.; Scalmani, G.; Barone, V.; Mennucci, B.; Petersson, G. A.; Nakatsuji, H.; Caricato, M.; Li, X.; Hratchian, H. P.; Izmaylov, A. F.; Bloino, J.; Zheng, G.; Sonnenberg, J. L.; Hada, M.; Ehara, M.; Toyota, K.; Fukuda, R.; Hasegawa, J.; Ishida, M.; Nakajima, T.; Honda, Y.; Kitao, O.; Nakai, H.; Vreven, T.; Montgomery, J. A., Jr.; Peralta, J. E.; Ogliaro, F.; Bearpark, M.; Heyd, J. J.; Brothers, E.; Kudin, K. N.; Staroverov, V. N.; Kobayashi, R.; Normand, J.; Raghavachari, K.; Rendell, A.; Burant, J. C.; Iyengar, S. S.; Tomasi, J.; Cossi, M.; Rega, N.; Millam, N. J.; Klene, M.; Knox, J. E.; Cross, J. B.; Bakken, V.; Adamo, C.; Jaramillo, J.; Gomperts, R.; Stratmann, R. E.; Yazyev, O.; Austin, A. J.; Cammi, R.; Pomelli, C.; Ochterski, J. W.; Martin, R. L.; Morokuma, K.; Zakrzewski, V. G.; Voth, G. A.; Salvador, P.; Dannenberg, J. J.; Dapprich, S.; Daniels, A. D.; Farkas, Ö.; Foresman, J. B.; Ortiz, J. V.; Cioslowski, J.; Fox, D. J. *Gaussian 09*, Revision D.01; Gaussian, Inc.: Wallingford, CT, 2009.
(87) (a) Fukui, K. *Acc. Chem. Res.* **1981**, *14*, 363−368. (b) Hratchian, H. P.; Schlegel, H. B. In *Theory and Applications of Computational Chemistry: The First 40 Years*; Dykstra, C. E., Frenking, G., Kim, K. S., Scuseria, G., Eds.; Elsevier: Amsterdam, 2005; pp 195−249.
(88) (a) Miertuš, S.; Scrocco, E.; Tomasi, J. *Chem. Phys.* **1981**, *55*, 117−29. (b) Miertuš, S.; Tomasi, J. *Chem. Phys.* **1982**, *65*, 239−45. (c) Pascual-Ahuir, J. L.; Silla, E.; Tuñón, I. *J. Comput. Chem.* **1994**, *15*, 1127−38. (d) Cossi, M.; Barone, V.; Cammi, R.; Tomasi, J. *Chem. Phys. Lett.* **1996**, *255*, 327−35. (e) Cossi, M.; Barone, V.; Mennucci, B.; Tomasi, J. *Chem. Phys. Lett.* **1998**, *286*, 253−60. (f) Cossi, M.; Scalmani, G.; Rega, N.; Barone, V. *J. Chem. Phys.* **2002**, *117*, 43−54.
(89) Kozuch, S.; Martin, J. M. L. *J. Comput. Chem.* **2013**, *34*, 2327−2344.
(90) Kozuch, S.; Martin, J. M. L. *Phys. Chem. Chem. Phys.* **2011**, *13*, 20104−20107.
(91) (a) Neese, F. *ORCA − An ab Initio, Density Functional and Semiempirical Program Package*, V. 3.0 (Rev. 2); MPI für Chemische Energiekonversion: Mülheim a. d. Ruhr, Germany, 2013. (b) Neese, F. *WIREs Comput. Mol. Sci.* **2012**, *2*, 73.
(92) (a) Baerends, E. J.; Ellis, D. E.; Ros, P. *Chem. Phys.* **1973**, *2*, 41. (b) Dunlap, B. I.; Connolly, J. W. D.; Sabin, J. R. *J. Chem. Phys.* **1979**, *71*, 3396. (c) Van Alsenoy, C. *J. Comput. Chem.* **1988**, *9*, 620. (d) Kendall, R. A.; Früchtl, H. A. *Theor. Chem. Acc.* **1997**, *97*, 158. (e) Eichkorn, K.; Treutler, O.; Öhm, H.; Häser, M.; Ahlrichs, R. *Chem. Phys. Lett.* **1995**, *240*, 283. (f) Eichkorn, K.; Weigend, F.; Treutler, O.; Ahlrichs, R. *Theor. Chem. Acc.* **1997**, *97*, 119. (g) Whitten, J. L. *J. Chem. Phys.* **1973**, *58*, 4496.
(93) Weigend, F. *Phys. Chem. Chem. Phys.* **2006**, *8*, 1057.
(94) Hättig, C. *Phys. Chem. Chem. Phys.* **2005**, *7*, 59. Hellweg, A.; Hättig, C.; Höfener, S.; Klopper, W. *Theor. Chem. Acc.* **2007**, *117*, 587.
(95) Riplinger, C.; Sandhoefer, B.; Hansen, A.; Neese, F. *J. Chem. Phys.* **2013**, *139*, 134101. Miller, J. L. *Phys. Today* **2013**, *66*, 15.
(96) (a) Reed, A. E.; Curtiss, L. A.; Weinhold, F. *Chem. Rev.* **1988**, *88*, 899−926. (b) Glendening, G. E. D.; Badenhoop, J. K.; Reed, A. E.; Carpenter, J. E.; Bohmann, J. A.; Morales, C. M.; Weinhold, F. *NBO 5*; Theoretical Chemistry Institute,University of Wisconsin: Madison, WI, 2001; http://www.chem.wisc.edu/~nbo5.
(97) Keith, T. A.*AIMAll*, Version 13.02.26; TK Gristmill Software: Overland Park, KS, USA, 2012; aim.tkgristmill.com.

DOI: 10.1021/ic502832j
Inorg. Chem. 2015, 54, 2253−2263